

## Submicrometre Beams from a Hard X-ray Waveguide at a Third-Generation Synchrotron Radiation Source

A. Cedola,<sup>a</sup> S. Lagomarsino,<sup>b</sup> S. Di Fonzo,<sup>c</sup> W. Jark,<sup>c</sup> C. Riekel<sup>a\*</sup> and P. Deschamps<sup>a</sup>

<sup>a</sup>European Synchrotron Radiation Facility, BP 220, F-38043 Grenoble CEDEX, France,

<sup>b</sup>Istituto di Elettronica dello Stato Solido-CNR, via Cineto Romano 42, I-00156 Roma,

Italy, and <sup>c</sup>Sincrotrone Trieste, Padriciano 99, I-34012 Trieste, Italy. E-mail: riekel@esrf.fr

(Received 13 December 1996; accepted 15 August 1997)

The use of an X-ray waveguide for scattering experiments at an undulator of a third-generation synchrotron radiation source is discussed. The performance with a perfect crystal monochromator, multilayer monochromator and focusing mirror is explored. A maximum flux of  $8 \times 10^9$  photons  $s^{-1}$  at  $\lambda = 0.083$  nm was obtained for a  $0.15$  (V)  $\times$   $600$  (H)  $\mu m^2$  beam at the exit of the waveguide with a multilayer monochromator. The combination of an Si (111) monochromator and ellipsoidal mirror resulted in a flux of  $\sim 10^9$  photons  $s^{-1}$  but with a horizontal compression of the beam to  $\sim 30$   $\mu m$ . The use of the waveguide in diffraction experiments is addressed.

**Keywords:** microbeams; X-ray diffraction.

### 1. Introduction

There is currently an intense interest in developing submicrometre beams at third-generation synchrotron radiation sources in the hard X-ray regime for applications in diffraction, fluorescence or imaging. Optical systems for which submicrometre beams with monochromatic radiation have been demonstrated are mirrors (Iida & Hirano, 1996), multilayer mirrors (Thompson & Chapman, 1996), Fresnel zone plates (Suzuki *et al.*, 1997), tapered glass capillaries (Thiel, Bilderback, Lewis & Stern, 1992), Bragg–Fresnel optics (Kuznetsov, Snigireva, Snigirev, Engström & Riekel, 1994) and X-ray waveguides (Spiller & Segmüller, 1974; Feng, Sinha, Deckman, Hastings & Siddons, 1995; Lagomarsino *et al.*, 1996; Jark *et al.*, 1996). Research and development in optics and practical applications are required for all of these systems in order to optimize their performance.

In this article experience obtained with a waveguide at an undulator beam of the European Synchrotron Radiation Facility (ESRF) is discussed. Different types of monochromators [Si (111); W/Si multilayers] are explored and the combination of a waveguide with a focusing mirror is demonstrated. Finally, practical experience with diffraction experiments is reported.

### 2. X-ray waveguide optics

X-ray waveguide optics are of interest due to a compression of the beam in one direction which distinguishes them from slit systems. The present waveguide structure was prepared by sputtering a carbon–chromium sandwich structure on a glass substrate (Fig. 1). A resonance phenomenon for an

incident X-ray beam occurs when the standing wave, which has been established in the carbon layer due to total reflection from the underlying chromium layer, has a periodicity which is an integer fraction of the thickness of the layer (Lagomarsino *et al.*, 1996; Jark *et al.*, 1996). Several resonance modes can therefore be created, each one at a specific incident angle. In resonance the intensity of the field inside the layer is 10–100 times higher than the incident beam intensity. The resonance modes can propagate through the carbon layer with the energy flow confined between the carbon interfaces. For higher-order modes the beam size at the exit will at most correspond to the layer thickness, while for the fundamental mode the full width at half maximum (FWHM) of the intensity distribution is only half of this thickness. Best trapping of the intensity [resonant beam coupling (RBC)] is achieved if the carbon resonator layer is covered with a thin 4.4 nm chromium layer. In this case the evanescent wave in the metal layer couples most efficiently with the response. The last 2 mm in

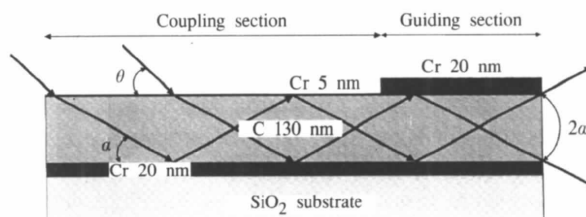


**Figure 1**

Schematic design of the waveguide structure.  $\theta$  is the incidence angle on the waveguide surface; the incidence angle  $\alpha$  on the interior Cr surface of the waveguide differs from  $\theta$  due to the refraction in the film.

the termination part of the waveguide are covered with an opaque metal layer, such that the beam is only guided and no intensity leaks back to above the guide, where it may interfere with the exiting beam.

In a previous experiment with a monochromatic beam from an Si (111) channel-cut monochromator it was shown that a 0.13  $\mu\text{m}$ -thick pencil-shaped beam can be obtained with such a structure for several resonance orders (Jark *et al.*, 1996). As a result of the geometry, two beams exit from the waveguide which are separated by an angle  $2\alpha$  (Lagomarsino *et al.*, 1996; Feng *et al.*, 1995; Jark *et al.*, 1996), where  $\alpha$  increases with the order of resonance. Each of the two beams is slightly divergent due to diffraction of the radiation at the waveguide exit. At a wavelength of  $\lambda = 0.095$  nm and a layer thickness of 0.15  $\mu\text{m}$  this divergence is 0.9 mrad (Jark *et al.*, 1996). It has also been shown that the two beams exiting from the waveguide are highly coherent for every order (Feng *et al.*, 1995; Jark *et al.*, 1996). This implies that the roughness at the interfaces does not give rise to a significant degradation of phase coherence of the waveguided field.

### 3. Experimental

Experiments were performed on the microfocus beamline at the ESRF (Fiedler, Engström & Riekkel, 1995). The photon source parameters of the low- $\beta$  undulator are given in Table 1. The three different optics used were (i) an Si (111) monochromator at  $\lambda = 0.095$  nm with  $\Delta\lambda/\lambda = 2 \times 10^{-4}$ , (ii) a W/Si multilayer double monochromator (Deschamps *et al.*, 1995) at  $\lambda = 0.083$  nm with  $\Delta\lambda/\lambda \simeq 10^{-1}$ , and (iii) an Si (111) monochromator at  $\lambda = 0.095$  nm used in combination with an ellipsoidal mirror (Fiedler *et al.*, 1995). In this last case the waveguide was placed at the focal spot of the mirror. Scattered radiation was suppressed at the focal position by a collimator of 30  $\mu\text{m}$  diameter which transmits practically the full focused beam. In all cases the same waveguide (see above) was used.

With a focusing ratio of 10:1 for the ellipsoidal mirror, the divergence of the beam at the sample position is obtained directly from the source parameters: 208 (H)  $\times$  17 (V)  $\mu\text{rad}^2$ . For the case of the unfocused beam with the Si (111) or the multilayer monochromator, the beam size in front of the waveguide was limited by slits to about 600 (H)  $\times$  65 (V)  $\mu\text{m}^2$ . Then, if the monochromator does not alter the beam divergence, this slit limits the accepted beam divergence to  $(s + S)/D$ , where  $s$  is the source size,  $S$  is the slit setting and  $D$  is the source distance. Consequently, one finds 22 (H)  $\times$  2.6 (V)  $\mu\text{rad}^2$ . With the waveguide compressing the beam only in the vertical direction, the different values for the horizontal divergence do not affect its performance. Instead, the vertical beam divergence needs to be considered. Theoretically, the angular acceptance of the waveguide, assuming zero roughness at the interfaces, is 2.6  $\mu\text{rad}$  for the first resonance mode, 5.8  $\mu\text{rad}$  for the second and 10.8  $\mu\text{rad}$  for the third. These values are larger than the expected beam divergence and consequently no

**Table 1**

Photon source parameters of the low- $\beta$  undulator.

	Horizontal	Vertical
Size (FWHM) ( $\mu\text{m}$ )	134	24
Divergence (FWHM) ( $\mu\text{rad}$ )	208	17

correction for the latter should have to be applied. However, this is in contradiction with the experimental data, where the following angular ranges were found for the FWHM of the excitation of the different orders (see Jark *et al.*, 1996; Fig. 2: 16  $\mu\text{rad}$  for the first resonance, 17  $\mu\text{rad}$  for the second and 22  $\mu\text{rad}$  for the third). A deconvolution of the ideal waveguide acceptance will leave a divergence of about 16  $\mu\text{rad}$ . Whether this needs to be assigned to a divergence increase in the crystal monochromator or to an acceptance broadening due to imperfections in the waveguide structure is not clear at this point. The fundamental mode travels with the smallest internal angle and should thus be the most intense at the waveguide exit. The observation of almost equal intensities exiting in the first three guided modes would thus actually favour the first argument, and would indicate an undesirable mismatch between the waveguide acceptance and the beam divergence.

The mismatch is even worse in the case of the focused beam, in which the vertical divergence of 170  $\mu\text{rad}$  exceeds by far the waveguide acceptance.

### 4. Results and discussion

#### 4.1. Efficiency of the waveguide

The following photon fluxes were observed behind the waveguide in the different experimental conditions:

(i)  $5 \times 10^8$  photons  $\text{s}^{-1}$  in an unfocused beam from an Si (111) crystal and by use of the above-mentioned slit of 65  $\times$  600  $\mu\text{m}^2$ ;

(ii)  $8 \times 10^9$  photons  $\text{s}^{-1}$  for a multilayer monochromator instead of the Si (111) crystal under the same conditions as (i);

(iii)  $1 \times 10^9$  photons  $\text{s}^{-1}$  in a focused beam with Si (111) crystals and a beam collimator of 30  $\mu\text{m}$  diameter.

As will be shown below, only in case (i) was a single mode exiting the waveguide for a particular angle of incidence. In the case of large-band-pass multilayers [case (ii)] several modes were always exited. The same holds for a large beam divergence due to focusing [case (iii); unpublished]. Consequently, only in case (i) does one find transverse spatially coherent radiation at the exit of the waveguide. Here the resulting photon flux corresponds to a transmission coefficient through the waveguide of 0.002. With this information one can now discuss the performance of the waveguide in comparison with expectations.

We start from the consideration that the further in front of the guiding section a photon impinges onto the waveguide, the more likely it is to be absorbed and to be subject to losses in the internal reflection processes. By performing

'ray-tracing' calculations one finds that a zero-size beam has a transmission coefficient through the guiding section of 0.53 (unpublished). The same beam vertically translated by  $5\ \mu\text{m}$  would have half the probability to exit. Thus, the vertical width which effectively contributes to the outgoing flux is about  $15\ \mu\text{m}$ , and a  $65\ \mu\text{m}$  beam, such as we had in our experiment, will only have a transmission of 0.05. If one considers the above possible mismatch in angular acceptance of about a factor of five, one could at best expect a transmission coefficient of 0.01. Thus, the experimental value of 0.002 still gives some margin for future improvement in the efficiency. Better transmission should be achievable with better waveguides and with better matching between the waveguide phase-space acceptance and the incident beam size and divergence. (*Note added in proof*: a factor of three has already been gained in the meantime; to be published in *Applied Physics Letters*.)

#### 4.2. Spectral throughput

The reflectivity curve was determined from an angular scan of the waveguide with a pin diode as detector. Fig. 2 shows a comparison between reflectivity curves obtained with the beam from the channel-cut Si (111) monochromator and from the W/Si multilayers. Owing to the larger band pass the minima for the multilayer beam are larger and more shallow with respect to those obtained with the monochromatic beam. This can be explained by the fact that the resonances have a very small intrinsic angular width, but a wavelength-dependent angular position.

An even more dramatic effect is evident in the analysis of the beam exiting from the waveguide. The intensity of the exit beam is shown in Fig. 3 for the Si (111) beam and for the W/Si multilayers where a large broadening and overlap

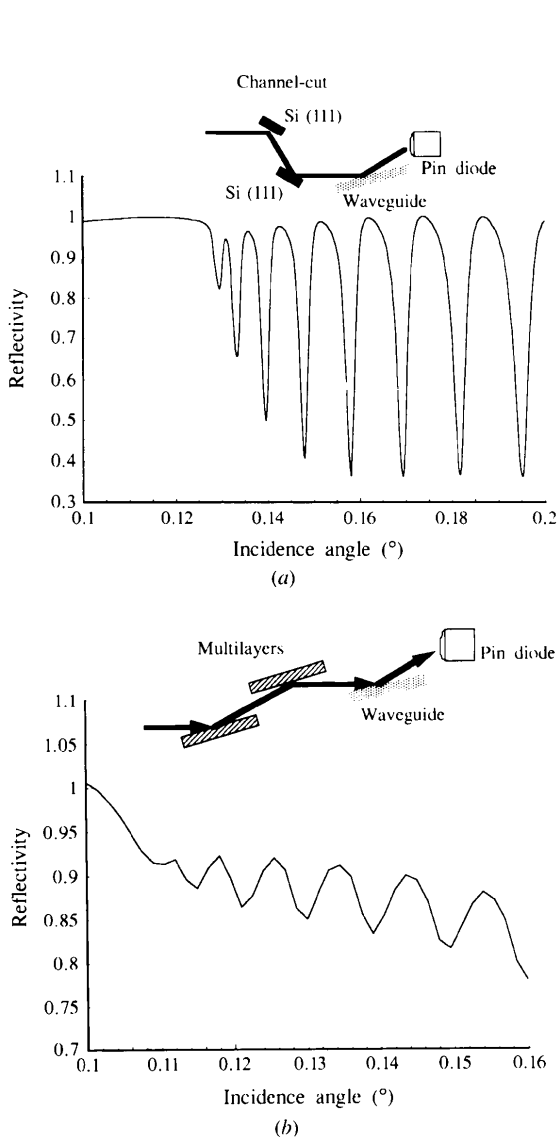


**Figure 2**  
(a) Reflectivity curve of the waveguide with the Si(111) monochromator. (b) Reflectivity curve of the waveguide with W/Si multilayers.

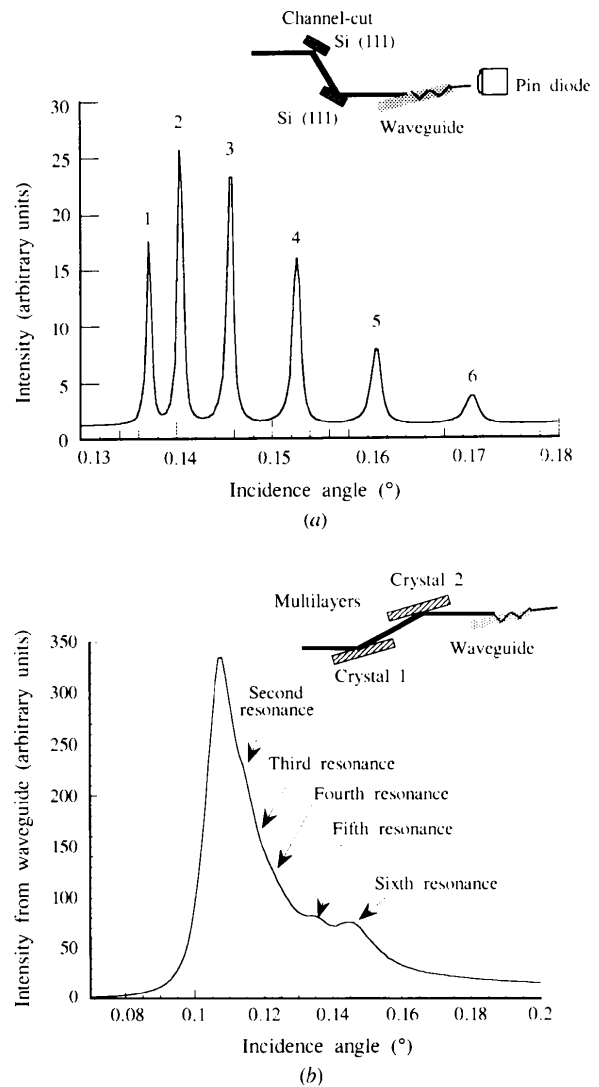


**Figure 3**  
(a) Intensity at the exit of the waveguide with a beam from an Si (111) monochromator. (b) Intensity at the exit of the waveguide with a W/Si multilayer beam. Intensities from the Si (111) beam have been scaled to the multilayer curve by taking the ratio of the photodiode output into account.

between the resonance maxima are clearly visible. For the multilayer beam it is expected that mode mixing will take place, *i.e.* the simultaneous excitation, for the same nominal incident angle, of more than one resonance. This is due to the combined effect of finite divergence and spectral width of the incoming beam.

In order to test the spectral throughput of the waveguide for the multilayer beam, the incidence angle was selected for the second order of resonance and the spectrum at the exit of the waveguide was analyzed by an Si (111) crystal. Fig. 4 shows the spectrum before and after the waveguide. The two spectra are quite similar suggesting that the waveguide transmits most of the spectrum. Some differences exist, however, due to the following:

(i) The two beams exiting from the waveguide are separated by an angle  $2\alpha_2$  (the subscript refers to the order of resonance). Both beams carry the energy spectrum of the

incoming beam and add their intensity in the resulting spectrum. This geometric effect results in an angular broadening.

(ii) Mode mixing gives rise to beams exiting from the waveguide where minor contributions from the first and third orders add to the second order of resonance. As a consequence, additional pairs of beams, separated by angles  $2\alpha_1$  and  $2\alpha_3$ , emanate from the waveguide. These beams also contribute to the total final spectrum with their relative angular shifts.

#### 4.3. Application examples

In order to avoid a significant spreading of the beam, samples have to be brought close ( $<100\ \mu\text{m}$ ) to the exit of the waveguide. Diffraction patterns can be obtained after proper shielding of background scattering from surface and fluorescent radiation coming from the waveguide ( $\text{Cr } K\alpha$ :  $0.23\ \text{nm}$ ) by a heavy metal cover.

Fig. 5 shows a diffraction pattern of  $\alpha\text{-Al}_2\text{O}_3$  powder recorded in 30 s with the multilayer beam using a liquid-nitrogen-cooled CCD at  $\sim 85\ \text{mm}$  from the sample (Koch, 1994). The profile of the (104) reflection in a radial direction reflects the wavelength spectrum of the multilayers (Fig. 4).

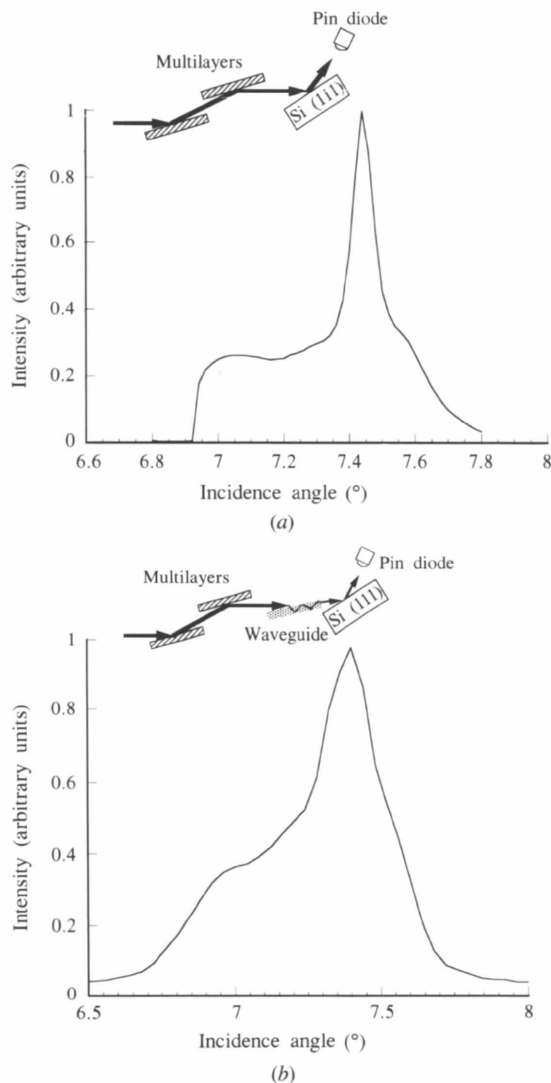


**Figure 4**  
(a) Wavelength spectrum of the multilayer beam determined by an Si (111) rocking curve. (b) Wavelength spectrum of the multilayer beam at the exit of the waveguide.

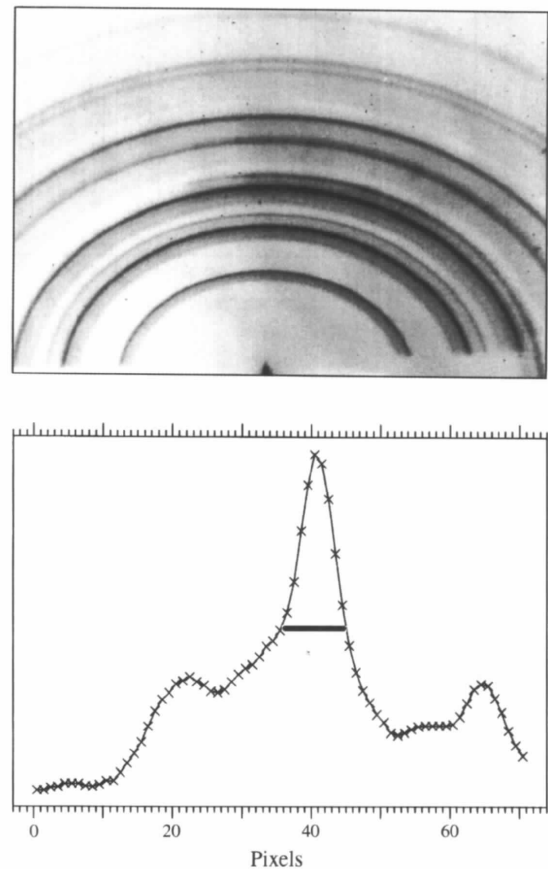


**Figure 5**  
 $\alpha\text{-Al}_2\text{O}_3$  diffraction pattern obtained with the multilayer beam at the exit of the waveguide. The bar in the central peak corresponds to  $\Delta s \approx 0.28\ \text{nm}^{-1}$ . The lower diagram shows a radial scan of the (104) reflection.

Fig. 6 shows the diffraction pattern of a  $\sim 100\ \mu\text{m}$ -thick hexacosane paraffin sample,  $\text{CH}_3(\text{CH}_2)_{24}\text{CH}_3$ , recorded with the monochromatic beam. The rather low detector quantum efficiency of  $\sim 0.3$  required 2 min exposure time. Peak shapes are regular in this case with  $\Delta s = 0.027\ \text{nm}^{-1}$  (FWHM) for the (111) reflection while the FWHM of the central feature in Fig. 5 corresponds roughly to  $\Delta s = 0.28\ \text{nm}^{-1}$ . This difference reflects the difference in bandpass. There is, however, residual scattering around the primary beam which could not be removed with the present shielding. The origin of the grainy structure in the background is not clear at present but could be due to hard X-ray background noise in the experimental hutch or residual impurities in the sample. This structure is visible due to the very low intrinsic noise level of the detector corresponding to about ten X-ray photons under the experimental conditions.

## 5. Conclusions

The status of X-ray waveguides for microbeam experiments using a high-brilliance insertion device has been summarized.  $5 \times 10^8\ \text{photons s}^{-1}$  have been obtained at the exit of the waveguide in a  $0.13\ (\text{V}) \times 600\ (\text{H})\ \mu\text{m}$  beam monochromatized by an Si (111) crystal. The flux increases to  $1 \times 10^9\ \text{photons s}^{-1}$  in a beam focused by an ellipsoidal

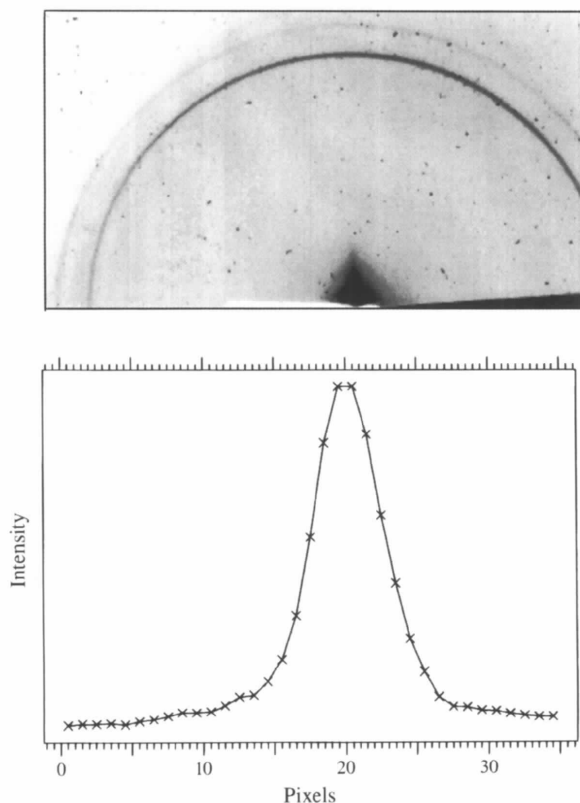


**Figure 6** Diffraction pattern from a  $\sim 100\ \mu\text{m}$ -thick paraffin sample obtained with an Si (111) beam at the exit of the waveguide. The lower diagram shows a radial scan of the (111) reflection.

mirror and to  $8 \times 10^9\ \text{photons s}^{-1}$  for an unfocused beam from a multilayer monochromator instead of the Si (111) crystal. With the parameters of the present waveguide a hypothetical slit of the same size would give approximately the same flux. However, an improvement in intrinsic efficiency is highly probable. Furthermore, beyond the fact that such a slit does not yet exist, it would have strong Fraunhofer diffraction. The waveguide under consideration instead would have much weaker fringes (Jark *et al.*, 1996). Beyond this fact, interest in such a device is also based on their divergence and coherence properties: in fact the divergence of the exit beam, in the Si monochromator case, is relatively small ( $\sim 1\ \text{mrad}$ ), and therefore useful for high-resolution diffraction studies. Furthermore, as discussed by Jark *et al.* (1996), the exit beam is highly coherent and therefore of high interest for hard X-ray phase-contrast experiments (*e.g.* Raven *et al.*, 1996; Cloetens, Barret, Baruchel, Guigay & Schlenker, 1996) and X-ray photon correlation spectroscopy. From this point of view it is interesting to note that the highest flux has been obtained with a multilayer beam, but at the expense of the coherence properties, because in this case mode mixing occurs which can have negative consequences on the coherence of the two beams (Born & Wolf, 1980). A focusing optic in front of the waveguide is useful in order to increase the flux density at the exit of the waveguide. The presently used ellipsoidal mirror could be replaced by a Kirkpatrick–Baez-type mirror system which should, in principle, allow an increase of the total efficiency and a reduction of the horizontal beam size to the micrometre range.

Various sources of background can be largely suppressed by proper shielding. Work is in progress to integrate shielding directly into the waveguide structure. For diffuse scattering applications one will, however, have to explore waveguide structures with a low intrinsic scattering background. Thus, an Mo/C waveguide structure would allow the suppression of the fluorescent background for the wavelength used in the present case (Mo  $K\alpha$ : 0.07 nm).

One of us (AC) wishes to acknowledge financial support by INFM (Genova, Italy) for staying at the ESRF.

## References

- Born, M. & Wolf, E. (1980). *Principles of Optics*, 6th ed. Oxford: Pergamon.
- Cloetens, P., Barret, R., Baruchel, J., Guigay, J. P. & Schlenker, M. (1996). *J. Phys. D*, **29**, 133–146.
- Deschamps, P., Engström, P., Fiedler, S., Riekkel, C., Wakatsuki, S., Høghøj, P. & Ziegler, E. (1995). *J. Synchrotron Rad.* **2**, 124–131.
- Feng, Y. P., Sinha, S. K., Deckman, H. W., Hastings, J. B. & Siddons, D. P. (1995). *Appl. Phys. Lett.* **67**(24), 3647–3649.
- Fiedler, S., Engström, P. & Riekkel, C. (1995). *Rev. Sci. Instrum.* **66**, 1348–1350.
- Iida, A. & Hirano, K. (1996). *Nucl. Instrum. Methods*, **B114**, 149–153.
- Jark, W., Di Fonzo, S., Lagomarsino, S., Cedola, A., di Fabrizio, E., Bram, A. & Riekkel, C. (1996). *J. Appl. Phys.* **80**, 4831–4836.

- Koch, A. (1994). *Nucl. Instrum. Methods*, **A348**, 654–658.
- Kuznetsov, S. M., Snigireva, I. I., Snigirev, A. A., Engström, P. & Riekel, C. (1994). *Appl. Phys. Lett.* **65**, 827–829.
- Lagomarsino, S., Jark, W., Di Fonzo, S., Cedola, A., Mueller, B. R., Riekel, C. & Engström, P. (1996). *J. Appl. Phys.* **79**, 4471–4473.
- Raven, C., Snigirev, A. A., Snigireva, I. I., Spanne, P., Souvorov, A. & Kohn, V. (1996). *Appl. Phys. Lett.* **69**(13), 1826–1828.
- Spiller, E. & Segmüller, A. (1974). *Appl. Phys. Lett.* **24**(1), 60–61.
- Suzuki, Y., Kamijo, N., Tamura, S., Handa, S., Takeuchi, A., Yamamoto, S., Sugiyama, H., Ohsumi, K. & Ando, M. (1997). *J. Synchrotron Rad.* **4**, 60–63.
- Thiel, D. J., Bilderback, D. H., Lewis, A. & Stern, E. A. (1992). *Nucl. Instrum. Methods*, **A317**, 597–600.
- Thompson, A. C. & Chapman, K. (1996). *Applications of Synchrotron Radiation Techniques to Materials Science*, Vol. 3, edited by L. J. Terminello, S. M. Mini, H. Ade & D. L. Perry. *Mater. Res. Soc. Symp. Proc.* Vol. 437.